J. Anat. (2018) 233, pp 177-192

The cellular localization and redistribution of multiple aquaporin paralogs in the spermatic duct epithelium of a maturing marine teleost

François Chauvigné[1], Janmejay Parhi[2], Carla Ducat[1], Judith Ollé[1], Roderick Nigel Finn[1,3] and Joan Cerdà[1]

[1] *IRTA-Institut de Ciències del Mar, Consejo Superior de Investigaciones Científicas (CSIC), 08003 Barcelona, Spain*
[2] *Fish Genetics and Reproduction Department, College of Fisheries, Central Agricultural University, Lembucherra, 799210, Tripura, India*
[3] *Department of Biological Sciences, Bergen High Technology Centre, University of Bergen, 5020 Bergen, Norway*

Correspondence
Joan Cerdà, IRTA-Institut de Ciències del Mar, Consejo Superior de Investigaciones Científicas (CSIC), 08003 Barcelona, Spain. T: +34 932309531; E: joan.cerda@irta.cat

Abstract

Aquaporin-mediated fluid transport in the mammalian efferent duct and epididymis is believed to play a role in sperm maturation and concentration. In fish, such as the marine teleost gilthead seabream (*Sparus aurata*), the control of fluid homeostasis in the spermatic duct seems also to be crucial for male fertility, but no information exists on the expression and distribution of aquaporins. In this study, RT-PCR and immunoblotting analyses, employing available and newly raised paralog-specific antibodies for seabream aquaporins, indicate that of up to nine functional aquaporins, Aqp0a, -1aa, -1ab, -3a, -4a, -7, -8bb, -9b and -10b, are expressed in the spermatic duct. Immunolocalization of the channels in the resting spermatic duct reveals that Aqp0a, -1aa, -4a, -7 and -10b are expressed in the monolayered luminal epithelium, Aqp8b and -9b in smooth muscle fibers, and Aqp1ab and -3a in different interstitial lamina cells. In the epithelial cells, Aqp0a and -1aa are localized in the short apical microvilli and Aqp4a and -10b show apical and basolateral staining, whereas Aqp7 is solely detected in vesicular compartments. Upon spermiation, an elongation of the epithelial cells sterocilia, as well as the folding of the epithelium, is observed. At this stage, single and double immunostaining, using two aquaporin paralogs or the Na^+/K^+-ATPase membrane marker, indicate that Aqp1ab, -3a, -7, -8bb and -9b staining remains unchanged, whereas in epithelial cells Aqp1aa translation is supressed, Aqp4a internalizes, and Aqp0a and -10b accumulates in the apical, lateral and basal plasma membrane. These findings uncover a cell type- and region-specific distribution of multiple aquaporins in the piscine spermatic duct, which shares conserved features of the mammalian system. The data therefore suggest that aquaporins may play different roles in the regulation of fluid homeostasis and sperm maturation in the male reproductive tract of fish.

Key words: sperm duct, sperm, water channel, aquaglyceroporin, glycerol, immunolocalization

Introduction

Once sperm is formed and released into the lumen of mammalian testicular seminiferous tubules, it is transported through a complex system of ducts, which allows its storage and maturation. In such species, the sperm acquires its motile and fertile properties during the long journey that begins in the efferent duct, which connects the rete testis with the initial section of the epididymis, and continues through the epididymis, which is a tightly-coiled tubular network that ends in the vas deferens (Robaire et al. 2006; Cornwall & Horsten, 2007). Anatomically, the epithelium of the efferent duct, epididymis and vas deferens is classified as pseudostratified and composed predominantly of columnar ciliated cells and basal cells, together with some non-ciliated, secretory cells (Hess, 2002). These epithelial cells are characterized by long non-motile stereocilia, which aid in the absorption of water to assist sperm transport and seminal fluid formation. The epithelium is surrounded by smooth muscle, which by its contractions further promotes sperm movement through the ducts.

In teleost fishes, the testicular efferent duct system also plays a role in the storage, nutrition and maturation of spermatozoa (Lahnsteiner, 2003). However, in these species this system is thought to originate from somatic cells of the gonad and/or the coelomic epithelium (reviewed in Nagahama, 1983) and is less complex and smaller than in mammals, being composed by a short testicular main duct connected to the spermatic duct (Billard, 1986; Lahnsteiner, 1993ab, 1994, 2003). Histologically, the testicular main duct epithelium is formed by an unfolded monolayer of columnar cells that can show secretory activity, whereas the spermatic duct epithelium can vary between species from a monolayered unfolded epithelium to a multilayered and folded epithelium, the latter increasing the internal surface of the spermatic duct (Lahnsteiner, 1993ab, 1994, 2003). As in mammals, the epithelial cells of the spermatic duct are generally ciliated (Meneguelli De Souza et al. 2015; Melo et al. 2016), and surrounded by a stroma containing smooth muscle cells that through their contraction facilitate sperm transport and expulsion (Walter et al. 2005).

In both mammals and teleosts, the acquisition and preservation of sperm viability and concentration within the sperm ducts until ejaculation are dependent on an adequate luminal environment (Lahnsteiner, 1993ab, 1994; Hess, 2002; Lahnsteiner, 2003). The seminal fluid is composed of additive products secreted from the sperm duct epithelial cells, such as glycogen, lipids, seminal plasma proteins or steroid glucuronides, required to nourish the sperm during its maturation (Turner, 1995; Lahnsteiner, 2003). In mammals, the efferent ducts are also the sites where up to 90% of the water coming from the seminiferous tubules is reabsorbed (Clulow et al. 1998; Dacheux & Dacheux, 2013), which concentrates the sperm in the initial segment of the epididymis and facilitates its interactions with the nourishing products. The control of fluid homeostasis in the sperm ducts thus appears to be crucial for male fertility.

In recent years, the role of molecular water channels, aquaporins, in the regulation of fluid transport in the male reproductive tract of mammals has been suggested (Huang et al. 2006; Da Silva et al. 2006b; Arrighi, 2014; Boj et al. 2015a). The aquaporins are small hydrophobic integral membrane proteins that allow the bidirectional movement of water and other small, uncharged solutes (i.e. glycerol, urea, carbon dioxide, nitric oxide, ammonia, hydrogen peroxide) across cell membranes following an osmotic gradient (King et al. 2004). In vertebrates, 17 different subfamilies of aquaporins have been found (Finn &

Cerdà, 2015, 2016), which can be divided into four major groups: the classical water-selective aquaporins (AQP0, -1, -2, -4, -5, -6, -14 and -15), the glycerol transporting aquaporins, known as aquaglyceroporins (AQP3, -7, -9, -10 and -13), the AQP8- and AQP16-types, and the unorthodox aquaporins (AQP11 and -12) (Finn et al. 2014, Finn & Cerdà, 2015, 2016). Immunolocalization studies have shown a diverse cell type- and region-specific expression of multiple aquaporins in the epithelial cells of the efferent ducts and epididymis in various mammalian species, apparently also showing interspecies differences (Boj et al. 2015a). Thus, AQP1 is present in the cilia of the efferent duct epithelial cells but not in the epididymal epithelium (Ford et al. 2014; Arrighi et al. 2016), while this channel is found in the apical membrane of endothelial cells in both regions (Badran & Hermo, 2002; Oliveira et al. 2005). In contrast, AQP9 is strongly expressed in the microvilli of nonciliated and ciliated cells of both the efferent duct and epididymis (Ruz et al. 2006; Hermo et al. 2008, 2011; Belleannée et al. 2009; Da Silva et al. 2006a; Domeniconi et al. 2008; Klein et al. 2013; Oliveira et al. 2013; Arrighi & Aralla, 2014). Interestingly, estrogens regulate the expression of AQP1 and -9 in the rat efferent duct epithelia (Pastor-Soler et al. 2002, 2010; Oliveira et al. 2005), and as a consequence, mice lacking the estrogen receptor alpha exhibit strong reduction of AQP1 and -9 expression in the efferent ducts leading to impaired water reabsorption, and a drop in sperm concentration and motility (Ruz et al. 2006). Other aquaporins have also been found in the sperm duct epithelium, such as AQP0, -2, -3, -5, -7, -8, -10 and -11, but their roles are not yet known (Hermo & Smith, 2011; Boj et al. 2015a). Nevertheless, the presence of different water-selective aquaporins and aquaglyceroporins in the efferent duct and epididymis epithelia suggests that a rapid movement of both water and other solutes between the lumen and the epithelial cells is required for sperm maturation.

In teleosts, however, only one study has reported the expression of an AQP10 ortholog, Aqp10b, in the spermatic duct of the marine teleost gilthead seabream (*Sparus aurata*) (Chauvigné et al. 2013). In this study, Aqp10b was immunolocalized in the apical membrane of unfolded and elongated luminal epithelial cells during the spermiation phase, which resembles the pattern of distribution of AQP10 in the rat efferent duct (Hermo et al. 2004). However, several other aquaporins investigated in the same study were not detected in the spermatic duct, which contrasts with the situation in the seabream testis where numerous aquaporins have been shown to be differently regulated during the reproductive cycle (Boj et al. 2015b). Therefore, the aim of the present work was to re-evaluate the expression of previously characterized aquaporin paralogs, Aqp0a, -1aa, -1ab, -7, -8bb, -9b and -10b, as well as additional aquaporins characterized here (Aqp3a and -4a), in the gilthead seabream spermatic duct at two different stages of the reproductive cycle (i.e. resting and spermiation). Our data reveal that multiple water-selective aquaporins and aquaglyceroporins are indeed expressed in the epithelial cells of the seabream spermatic duct as observed in mammals, with some paralogs being spatially redistributed in the plasma membrane upon spermiation. These findings suggest that aquaporins may play a role in the regulation of fluid homeostasis in the male reproductive tract of fish.

Materials and methods

Animals

Adult, farm-raised gilthead seabream males (2 years old) were maintained in the fish facility of the Institute of Marine Sciences, Spanish Council for Scientific Research (CSIC, Spain) following previously described procedures (Chauvigné et al. 2013; Boj et al. 2015b). During the resting and spermiation periods of the natural spawning season, fish were sedated with 500 ppm of phenoxyethanol (Sigma-Aldrich), weighted and immediately euthanized by decapitation. Biopsies of testes, spermatic ducts and other tissues were frozen in liquid nitrogen and stored at -80 °C for RNA and protein extraction, or processed for histology and immunofluorescence microscopy (see below). Procedures relating to the care and use of animals and sample collection were carried out in accordance with the protocols approved by the Ethics Committee (EC) of the Institut de Recerca i Tecnologia Agroalimentàries (IRTA, Spain) following the European Union Council Guidelines (86/609/EU). The present study was also specifically approved by IRTA EC.

Cloning of aquaporin-4a

Based on the sequences of partial cDNAs bearing the 5'- and 3'-UTRs encoding the gilthead seabream Aqp4a (GenBank accession numbers FM156410 and KC788198, respectively), gene-specific primers with *EcoR*V and *Spe*I restriction sites were designed to amplify the full-length cDNA (forward: 5´-gatatcGCTGCTGGATGCGATCCCGG-3´; reverse: 5´-actagtCTCGAGATGGATGCTCAAAAG-3´). Total RNA from ovarian samples was purified using the GenElute^{TM} mammalian total RNA miniprep kit (Sigma-Aldrich, St. Louis, MO, USA) according to the manufacturer's instructions, and cDNA synthesis was performed with 1 µg of total RNA using an oligo $dT_{(12-18)}$ primer and SuperScript II RT enzyme as previously described (Chauvigné et al. 2013). PCR was performed with the EasyA^{TM} high-fidelity PCR cloning enzyme (Agilent Technologies, Santa Clara, CA, USA) with an initial denaturing step for 2 min at 94°C, followed by 35 cycles of 94°C for 1 min, 60°C for 1 min, and 72°C for 2 min, ending with a final elongation at 72°C for 7 min. Subsequently, the full-length Aqp4a cDNA was cloned into the pGEM-T Easy vector (Promega Biosciences, LLC, San Luis Obispo, CA, USA) and sequenced by BigDye Terminator Version 3.1 cycle sequencing on ABI PRISM 377 DNA Analyser (Applied Biosystems, Life Technologies Corp., Carlsbad, CA, USA). The nucleotide sequence corresponding to the full-length Aqp4a cDNA was deposited in GenBank with accession number KY682700.

Antibodies

Production of polyclonal antisera for seabream Aqp3a, -4a and -10b were raised in rabbits or chickens against synthetic peptides corresponding to the C-terminus amino acid residues of the corresponding predicted proteins (Table 1) (Agrisera AB, Vännäs, Sweden). The antisera were purified by affinity chromatography against the synthetic peptides. Previously characterized antibodies against gilthead seabream Aqp0a, -1aa, -1ab, -7, -8bb and -9b were also employed (Table 1). The mouse monoclonal antibody ATP1A1 antibody (a5) against Na^+-K^+ ATPase (NKA) was purchased from the Developmental Studies Hybridoma Bank (University of Iowa, USA).

Functional expression in *Xenopus laevis* oocytes

Constructs for heterologous expression in *X. laevis* oocytes were generated by subcloning the full-length seabream aquaporin cDNAs into the pT7Ts expression vector. The cRNA synthesis and isolation of stage V-VI oocytes were carried out as previously described (Chauvigné et al. 2013). Oocytes were transferred to modified Barth's solution (MBS; 88 mM NaCl, 1 mM KCl, 2.4 mM $NaHCO_3$, 0.82 mM $MgSO_4$, 0.33 mM $Ca(NO_3)_2$, 0.41 mM $CaCl_2$, 10 mM HEPES, and 25 µg/ml gentamycin, pH 7.5) and injected with 50 nl of distilled water (negative control) or 50 nl of water solution containing 15 ng cRNA. The osmotic water permeability (P_f) of oocytes, as well as the uptake of radioactive [1,2,3-^{3}H]glycerol, were determined as previously described at pH 7.5 (Chauvigné et al. 2013). Experiments were carried out at least three times on different batches of

oocytes. Data (mean ± S.E.M.) were statistically analyzed by the one-way ANOVA, followed by the Duncan's multiple range test, using the Statgraphics Plus 4.1 software (Statistical Graphics Corp., USA). A P value < 0.05 was considered statistically significant.

RNA extraction and RT-PCR

Extraction of total RNA from different tissues (gills, lens, brain, spermatic duct, testis and sperm) and cDNA synthesis was carried out as described above. RT-PCR was performed using 1 µl of cDNA, EasyA™ high-fidelity PCR cloning enzyme and 0.5 µM of forward and reverse primers specific for each aquaporin paralog (Chauvigné et al. 2013). The amplification protocol was composed of an initial denaturing step for 2 min at 94°C, followed by 35 cycles of 94°C for 1 min, 60°C for 1 min, and 72°C for 2 min, ending with a final elongation at 72°C for 7 min. PCR products were run on 1% agarose gels.

Protein extraction and immunoblotting

Total membrane fractions of *X. laevis* oocytes were isolated as described previously (Kamsteeg & Deen, 2001). Seabream adult tissues (testis, spermatic duct, gills or kidney) were dissociated with a glass dounce homogenizer in ice-cold RIPA buffer containing 150 mM NaCl, 50 mM Tris-HCl, pH 8, 1% Triton X-100, 0.5% sodium deoxycholate, 1 mM EDTA, 1 mM EGTA, EDTA-free protease inhibitors (Roche Applied Science, Mannheim, Germany), 1 mM Na_3VO_4, and 1 mM NaF, and centrifuged at 14000 x *g* for 10 min at 4ºC. The supernatant was mixed with 2x Laemmli sample buffer containing 2M urea and 200 µM di-thiothreitol (DTT), heated at 95ºC for 10 min, aliquoted, deep frozen in liquid nitrogen, and stored at -80ºC.

For immunoblotting, total protein extracts were denatured at 95ºC for 10 min, electrophoresed in 12% SDS-PAGE, and blotted onto Immun-Blot® nitrocellulose 0.2 µm Membrane (Bio-Rad Laboratories Inc., Hercules, CA, USA) as previously described (Chauvigné et al. 2013). The membranes were blocked with 5% nonfat dry milk diluted in TBST (20 mM Tris, 140 mM NaCl, 0.1% Tween; pH 8) for 1 h at room temperature, and subsequently incubated overnight at 4ºC with the different aquaporin antibodies (1:1000) diluted in TBST with 5% nonfat dry milk. For the antibodies raised in chicken (Aqp3a and -4a), blocking and antibody dilution was realized with 1% milk and 1% BSA in TBST. Horseradish peroxidase (HRP)-coupled anti-rabbit or anti-chicken IgG secondary antibodies (sc-2004, Santa Cruz Biotechnology Inc., Dallas TX, USA; and PA1-28798, Thermo Fisher Scientific, Waltham, MA, USA, respectively) diluted in TBST+5% nonfat dry milk (1:5000) were added for 1 h at room temperature. Immunoreactive bands were revealed by the Immobilon™ Western chemiluminescent HRP substrate (Merck Millipore, Burlington, MA, USA).

Histological analysis

Isolated spermatic ducts were fixed in Bouin's fluid for 16 h at room temperature before being embedded in paraffin. Sections of ~7 µm in thickness were attached to UltraStick/UltraFrost Adhesion slides (Electron Microscopy Sciences, Hatfield, PA, USA) and stained with hematoxylin and eosin as previously described (Chauvigné et al. 2013).

Immunofluorescence microscopy

Tissues were fixed in 4% paraformaldehyde (PFA) for 6 h at room temperature and then washed, dehydrated, and embedded in paraffin. Sections of ~7 µm in thickness were attached to UltraStick/UltraFrost Adhesion slides and rehydrated before permeabilization with 0.1% Triton X-100 for 10 min at room temperature (for Aqp1aa, -1ab, -3a, -8bb, -9b and -10b), or cold acetone for 5 min (Aqp0a, -4a and -7). Sections were blocked in 5% goat serum and 0.1% BSA in PBS with

0.1% Tween-20 (PBST) for 1 h before incubation with the antibodies in PBST: 1:400 for Aqp1aa, -1ab, -7, -9b and -10b antibodies, 1:600 for Aqp0a and -8bb antibodies, 1:500 for Aqp3a and -4a antibodies, and 1:1000 for NKA antibody overnight at 4ºC. Slides mounted with adjacent sections were incubated with the antibodies preadsorbed with their respective immunizing peptides as negative controls. After washing, sections were incubated for 1 h at room temperature with either Alexa 488-coupled anti-rabbit IgG goat secondary antibody (1:1000; Thermo Fischer Scientific, A-11008) or Alexa 488-coupled anti-chicken IgY goat secondary antibody (1:2000; Thermo Fischer Scientific, A-11039) to detect aquaporins, or with Alexa 555-coupled anti-mouse IgG goat secondary antibody (1:1000; Thermo Fischer Scientific Corp., A-21422) to detect Na^+-K^+ ATPase. The nuclei were counterstained with 4',6-diamidino-2-phenylindole (DAPI, Sigma-Aldrich, D9564) at 1:3000 in PBS for 5 min, and slides were finally mounted using fluoromount aqueous anti-fading medium (Sigma-Aldrich). Sections were examined and photographed with a Zeiss Axio Imager Z1/ApoTome fluorescence microscope (Carl Zeiss Corp., Jena, Germany).

Double immunofluorescence was performed after blocking the sections with 5% goat serum and 0.1% bovine serum albumin for 1 h at room temperature, and incubation for another hour with PBS-diluted Aqp1aa, -7 or -8bb antisera (1:100), previously directly labeled with Alexa fluor 555 or Alexa fluor 488 dyes using the Zenon Alexa Fluor 555 or 488 Rabbit IgG Labeling Kits (Z-25305 and Z-25302, respectively; Thermo Fischer Scientific). Sections were then fixed in 4% PFA for 15 min before mounting in fluoromount aqueous anti-fading medium. Epifluorescence images were taken as described above.

Results

Functional characterization of gilthead seabream Aqp3a and -4a and antibody specificity

The permeation properties of the newly isolated gilthead seabream Aqp4a, as well as of the previously uncharacterized Aqp3a, were assessed using the *X. laevis* oocyte-swelling and radioactive glycerol uptake assays (Fig. 1A, B). Results show that both Aqp3a and -4a were able to conduct water but with different efficiency, while Aqp3a-injected oocytes show a ~3-fold increase in P_f with respect to the water-injected controls, Aqp4a expressing oocytes exhibit a ~10-fold increase in P_f (Fig. 1A). In contrast, isotope-labeled glycerol-uptake assays under isotonic conditions show that oocytes injected with Aqp3a are permeable to glycerol, the permeability being ~3 times higher than in the controls, whereas those expressing Aqp4a are not (Fig. 1B). These data confirm previous phylogenetic analysis (Finn et al. 2014), indicating that seabream Aqp3a is an aquaglyceroporin, while Aqp4a is a water-selective channel.

To subsequently investigate the expression and cellular localization of Aqp3a and -4a in the gilthead seabream spermatic duct, as well as that of Aqp10b, we produced affinity-purified antibodies against the C-terminus of these channels. The specificity of the antibodies for the corresponding paralog was tested by Western blot analysis on total membrane protein extracts from *X. laevis* oocytes expressing Aqp3a, -4a and -10b, as well as the other seabream aquaporins being investigated in this study (Aqp0a, -1aa, -1ab, -7, -8bb, and -9b) (Fig. 1C). The results show that each of the Aqp3a, -4a and -10b antisera generated specifically recognized its corresponding antigen, therefore indicating that these antibodies do not cross-react with any of the other aquaporins (Fig. 1C).

The cilia of the epithelial cells of the spermatic duct elongate during the spermiation period

Anatomical analysis confims that in the gilthead seabream the spermatic duct originates from the testicular main duct and ends in the gonopore (Fig. 2A, B). At the resting stage, the spermatic duct appears as a thin and translucent conduct with the lumen free of spermatozoa (Fig. 2A). During spermiation, coinciding with the strong increase in the size of the testis and the gonadosomatic index (Boj et al. 2015b), the spermatic duct becomes larger and longer and appears filled with sperm (Fig. 2B). Histological analyses on transversal sections of the spermatic duct reveal that at the resting stage the spermatic duct is composed by a monolayered unfolded epithelium external to a smooth muscle fibers array, where some dispersed interstitial/laminal cells are observed (Fig. 2C). At this stage, the epithelial cells show scarce sterocilia (microvilli) (Fig. 2C). In contrast, at the spermiating stage the height of the epithelium increases and folds, as the epithelial cells elongatedand exhibit cilia and vacuoles, probably reflecting the apocrine secretive stage of the cells (Fig. 2D). Trapped spermatozoa in the cilia can be observed in the vicinity of the epithelium (Fig. 2D).

Multiple aquaporins are expressed in the gilthead seabream spermatic duct

The expression of aquaporin genes in the spermatic duct at the resting and spermiation stages was assessed by RT-PCR using paralog specific primers. These experiments indicate that both water-selective aquaporins (*aqp0a*, *-1aa*, *-1ab*, *-4a* and *-8bb*) and aquaglyceroporins (*aqp3a*, *-7*, *-9b* and *-10b*) are positively expressed in the spermatic duct (Fig. 3A). In agreement with the mRNA data, protein products for all nine aquaporins are detected in protein extracts from the spermatic duct at the spermiation stage by SDS-PAGE and immunoblotting using the newly generated affinity-purified antibodies for Aqp3a, -4a and -10b, as well as antibodies for Aqp0a, -1aa, -1ab, -7, -8bb and -9b previously characterized (Fig. 3B). For Aqp8bb, a single immunoreactive band of approximately the same molecular mass as the predicted monomer is detected, whereas for all the other aquaporins additional secondary bands of higher molecular masses than the predicted monomers or smear patterns are revealed, which could correspond to dimerization products and/or complex posttranslational modifications (Fig. 3B). The specificity of the reactions was confirmed by the preadsorbtion of the antisera with the corresponding immunizing peptides (Fig. 3B).

Specific cellular localization of aquaporins in the gilthead seabream spermatic duct

The cellular localization of the nine aquaporins in the seabream spermatic duct at the resting and spermiation stages was determined by immunofluorescence microscopy using the paralog-specific antibodies. At the resting stage, Aqp0a is distributed mostly in the cytoplasm of the spermatic duct epithelial cells, although more accumulated protein is seen in regions surrounding the nuclei, while a faint Aqp0a staining is also detected in the apical plasma membrane (Fig. 4A). In contrast, Aqp1aa is solely and strongly expressed in the apical microvillar membranes of the epithelial cells (Fig. 4B), whereas the duplicate paralog Aqp1ab is exclusively detected in isolated interstitial cells embedded within the smooth muscle fiber cells, which based on their location could correspond to lymphocytes or macrophages (Fig. 4C). Aqp3a also appears associated to unidentified groups of cells deposited in the connective tissue beneath the epithelium, which show a granulated aspect (Fig. 4D). Finally, strong Aqp4a immunstaining is also detected in the apical and

basolateral plasma membranes of epithelial cells, as well as in the cytoplasm apparently with a homogeneous distribution (Fig. 4E).

During the spermiation stage, some paralogs, such as Aqp0a (Fig. 4K), Aqp1ab (Fig. 4M) and Aqp3a (Fig. 4N), maintain the same pattern of cellular localization in the epithelial and intertitial cells of the spermatic duct. However, Aqp1aa staining is no longer detected in the apìcal membrane of the epithelial cells, and it is only observed in the apical membrane of vascular endothelial cells (Fig. 4L, inset). Similarly, Aqp4a staining from the plasma membrane of epithelial cells seems to disappear, with the signal becoming localized in discrete cytoplasmic regions surrounding the nucleus (Fig. 4M).

To confirm the subcellular localization of Aqp0a and -4a in the spermatic duct epithelial cells during spermiation, we performed double immunostaining using an antibody against the NKA, which specifically labels the plasma membrane. These experiments confirm that Aqp0a is expressed both in the cytoplasm and the apical (stereocilia) and lateral plasma membrane of the epithelial cells, where it partially co-localizes with the NKA staining (Fig. 5A-C). In contrast, Aqp4a appears to localize preferentially in the basal cytoplasm of epithelial cells (Fig. 5D), when compared to the plasma membrane marker NKA (Fig. 5E), thus corroborating that Aqp4a expression in the plasma membrane is lost during spermiation.

The immunolocalization experiments for Aqp7, -8bb, -9b, and -10b in the gilthead seabream spermatic duct also reveals a different cellular distribution of these channels. In the resting spermatic duct, Aqp7 exhibits an intracellular expression in the epithelial cells, with the staining concentrated in dots close to the nuclei, suggesting its possible aggregation in vesicular compartments (Fig. 6A). In contrast, both Aqp8bb and -9b are exclusively observed in the smooth muscle fibers in a diffuse pattern (Fig. 6B, C), whereas Aqp10b is distributed within the cytoplasm and the apical and basolateral plasma membranes of epithelial cells (Fig. 6D), similarly to that found for Aqp4a. At the spermiating stage, the epithelial cells still express Aqp7, which remains in very discrete intracellular bundles (Fig. 6I), as well as Aqp10b, which shows a more evident expression in the membrane of the apical stereocilia (Fig. 6L). At this stage, the Aqp8bb and -9b staining remains unchanged in the smooth muscle fiber cells (Fig. 6J, K). Co-localization experiments of Aqp7 and -10b with the NAK in epithelial cells during spermiation confirms that Aqp7 exhibits a vesicular pattern within the cytoplasm (Fig. 7A-C), while Aqp10b is inserted in the apical plasma membrane and stereocilia (Fig. 7D-F).

Finally, to investigate whether Aqp0a, -4a, -7 and -10b are expressed in the same subcellular compartments of the spermatic duct epithelial cells during spermiation, double immunostaining experiments using paralog specific antibodies raised in different species were carried out. Interestingly, these trials show that Aqp0a and -4a do not colocalize within the epithelial cells, indicating that they were targeted to different intracellular compartments (Fig. 8C). On the contrary, Aqp4a and -7, both of which show a vesicular-type of intracellular staining, are indeed partially colocalized (Fig. 8F). Similar experiments for Aqp1ab and -3a reveal that these channels are expressed in different interstitial cells located in the connective tissue below the epithelium (Fig. 8G-I).

Altogether, the immunostaining data uncovers a complex pattern of expression of the nine aquaporin paralogs in the gilthead seabream spermatic duct which is depicted in Fig. 9. The scheme also summarizes the major changes in the subcellular distribution of the channels in the epithelial cells during spermiation: (i) the coordinated downregulation and internalization of Aqp1aa and -4a, respectively, and the accumulation of Aqp0a and -10b in

the apical, lateral and basolateral plasma membrane; and (ii) the prevalent retention of Aqp7 in intracellular vesicles.

Discussion

In teleost fish, a larger repertoire of aquaporins is found compared to mammals as a result of both tandem and genomic duplication events that arose early in the evolution of the lineage (Finn et al. 2014; Finn & Cerdà, 2015). Thus, most teleosts retain two or three genes within each aquaporin subfamily. Although many of the teleost aquaporins show comparable permeability properties to those of the mammalian orthologs (Tingaud-Sequeira et al. 2010; Cerdà & Finn, 2010; Engelund et al. 2013; Finn & Cerdà, 2015; 2016), as well as conserved tissue expression patterns in most cases, recent studies indicate that some duplicated teleost aquaporins are neofunctionalized (Tingaud-Sequeira et al. 2008; Finn & Cerdà, 2015; Cerdà et al. 2017). For example, Aqp1aa is ubiquitously expressed in almost all tissues, while Aqp1ab is accumulated in oocytes, where it plays a specific role mediating water uptake during meiosis associated oocyte hydration in marine teleosts producing pelagic eggs (Fabra et al. 2005; Zapater et al. 2011). Also, in the spermatozoa of marine fishes, Aqp1aa localizes along the flagellum and mediates water efflux during motility activation , whereas Aqp1ab is found predominantly in the spermatozoon head, and thus their roles during sperm activation have diverged (Chauvigné et al. 2013; Boj et al. 2015c).

In the present study, we show that multiple aquaporin paralogs, including Aqp0a, -1aa, -1ab, -3a, -4a, -7, -8bb, -9b and -10b, are differentially distributed in different compartments of the gilthead seabream spermatic duct. Such a divergent expression pattern has also been reported in mammals (Hermo & Smith, 2011; Boj et al. 2015a). In this work, however, we find that the epithelial cells of the seabream spermatic duct express Aqp0a, -1aa, -4a, -7 and -10b, while in most tetrapods, aquaporins with conserved substrate preferences, such as AQP1, -7 and -9, are detected in the epithelium of the efferent duct and/or epididymis (Hermo & Smith, 2011; Boj et al. 2015a). An exception to this is AQP2, which is accumulated in the epididymal epithelium in many species (Hermo & Smith, 2011; Boj et al. 2015a), but it is absent from the genomes of actinopterygian fishes (Finn et al. 2014). AQP0, which has only been reported to be expressed at low levels in epididymis epithelial cells of stallion (Klein et al. 2013) but not in rodents (Hermo et al. 2004; Da Silva et al., 2006a), and AQP4, are also exceptions. In the seabream, Aqp0a is found localized mostly in the cytoplasm and apical membrane of the spermatic duct epithelial cells, suggesting its role in fluid regulation across the epithelium. However, during spermiation Aqp0a is more prominent at the basolateral membrane of the epithelial cells, which may indicate the additional involvement of this channel in cell-to-cell adhesion structures, an important feature of columnar epithelial cells (Tang, 2017), at the time of sperm production. The dual function of mammalian and piscine AQP0 orthologs as water channel proteins and adhesion molecules has primarily been reported in lens fibers cells (Kumari & Varadaraj, 2009; Clemens et al. 2013; Chauvigné et al. 2016).

The expression of AQP1 in the apical membrane of the efferent duct epithelial cells is common among mammals, and in some species it is also found in the epididymis, whereas in the rat AQP3 localizes solely to basal cells of the epididymal epithelium that contact the basement membrane and do not extend to the epididymal lumen (Hermo & Smith, 2011; Boj et al. 2015a). The seabream Aqp1aa ortholog also shows a conserved localization in the

apical microvilli of the spermatic duct epithelium at the resting stage, whereas at spermiation this channel is no longer expressed by the epithelial cells and it appears only in the apical membrane of endothelial cells of blood vessels within the connective tissue, as previously reported in the rat (Badran & Hermo, 2002; Oliveira et al. 2005). However, the tandemly duplicated Aqp1ab paralog is exclusively expressed in dispersed interstitial lamina cells, that could represent lymphocytes or macrophages embedded within the connective tissue (Da Silva et al. 2011; Shum et al. 2014), which suggests the neofunctionalization of this channel in the seabream spermatic duct as observed in spermatozoa (Boj et al., 2015c). Interestingly, seabream Aqp3a is also expressed in other groups of interstitial cells not expressing Aqp1ab that are located close to the epithelium of the spermtic duct, but their identities are not yet known. Specific markers of the Aqp1ab- and -3a-expressing cells of the seabream spermatic duct would be necessary to uncover their identity and further unravel the role of these channels.

In contrast to reports for mammals, in this study we have obtained evidence for the expression of Aqp4a in the spermatic duct epithelium of seabream. This channel appears to be accumulated in the apical and basolateral plasma membranes of epithelial cells, whereas at spermiation Aqp4a is internalized from these membranes into intracellular storage vesicles. Thus, both Aqp1aa and -4a are removed from the plasma membrane of epithelial cells during spermiation, which suggests that these water-selective channels may not be required during spermiation and that other aquaporins, such as Aqp0a and -10b may take the water transport functions at this stage. However, the downregulation of Aqp1aa and -4a during the reproductive cycle differs. While Aqp1aa appears to be translationally supressed, the regulation of Aqp4a seems to occur at the posttranslational level. Both mechanisms could be under hormonal modulation, with estrogen and progestins being potential candidates, as they respectively regulate the expression of AQP1 and -9 in the rat efferent duct epithelia (Oliveira et al. 2005; Ruz et al. 2006; Pastor-Soler et al. 2010) and the process of spermiation in fish (Schulz et al. 2010; Scott et al. 2010). The endocrine regulation of aquaporins in the seabream spermatic duct, as well as the relevance of such regulation in semen physiology, is yet unknown and deserves further investigation.

A surprising finding of this study is that the expression of functional Aqp7 in the spermatic duct epithelial cells of the seabream remains intracellular, partially colocalizing with Aqp4a, irrespective of the stage of the reproductive cycle. This observation contrasts with data in rodents, where AQP7 is targeted to the basolateral membrane of the epididymal principal cells (Hermo et al. 2008). The stable localization of AQP7 in intracellular vesicles is unusual, but recent studies in mouse white adipose tissue have shown that this channel is re-localized to intracellular membranes of adipocytes in response to catecholamine-stimulated lipolysis, where it may affect the chemical equilibrium of lipolysis by reducing the local glycerol concentration around the endoplasmic reticulum and lipid droplets (Miyauchi et al. 2015). Therefore, it is possible that intracellular Aqp7 in the seabream epithelial cells of the spermatic duct plays a similar role controlling lipid metabolism to assist sperm maturation, but this hypothesis needs to be investigated.

In most mammals studied to date, the aquaglyceroporin AQP9 is highly abundant in the epididymal epithelium (Hermo & Smith, 2011; Arrighi, 2014; Boj et al. 2015a), where it is suggested to mediate the transport of glycerol as an aerobic metabolic substrate important for the maturation of spermatozoa (Cooper and Brooks, 1981; Da Silva et al. 2006b). In the seabream, however, the Aqp9b ortholog is not found in the epithelium of the spermatic duct but in the smooth muscle fibers, together with Aqp8bb. In contrast, in

mammals AQP9 is reported to be expressed in normal skeletal muscle fibers (Inoue et al. 2009; Wakayama et al. 2014), but not in smooth muscle cells, and both AQP8 and -9 have been observed in the developing masseter muscle (Wang et al. 2003). The roles of AQP9 and -8, and of the seabream Aqp9b and -8bb, in muscle cells are not known but they may be respectively involved in glycerol metabolism and the transport of reactive oxygen species (i.e. hydrogen peroxide) across the mitochondrial membranes to allow energy maintenance (Soria et al. 2010; Maeda 2012; Marchissio et al. 2012; Chauvigné et al. 2015).

Nevertheless, we confirm a previous study using a different antibody (Chauvigné et al. 2013) that the aquaglyceroporin Aqp10b, instead of Aqp9b, is expressed in the apical and basolateral plasma membrane of the seabream spermatic duct epithelium. This observation coincides with that described in the rat efferent duct where AQP10 is found in the microvilli of ciliated and non-ciliated cells of the epithelium (Hermo & Smith, 2011). The conserved expression of aquaglyceroporins in the epithelia of sperm ducts of mammals and seabream suggest that the transport of glycerol or other small neutral solutes is important for semen formation in fish and mammals. However, it has been reported that AQP9 knockout mice are fertile and show spermatozoa with normal motility (Rojek et al. 2007). These data imply that AQP9 is not essential for sperm physiology, but it cannot be ruled out compensatory regulation of glycerol transport by controlling the expression of other aquaglyceroporins such as AQP10 (Rojek et al. 2007; Verkman, 2009). Therefore, further studies are necessary to determine the role of the different aquaglyceroporins in the control of fluid transport in the sperm ducts.

In conclusion, by using immunohistochemical approaches, we established for the first time the presence of up to nine functional aquaporin paralogs in the spermatic duct of a teleost fish. Our data show a complex pattern of cellular and subcellullar localization and regulation of different water-selective aquaporins and aquaglyceroporins in the epithelial cells of the spermatic duct which resembles to that described in mammals. The findings suggest that transcellular water and nutrient transport pathways through aquaporins exist in the teleost spermatic duct epithelium, which likely play roles to assist the processes of sperm maturation and nutrition prior to ejaculation. Future studies will be necessary to ellucidate the specific regulation and physiological functions of the aquaporins in the spermatic duct of teleosts.

Acknowledgements

This work was supported by the CERCA Programme/Government of Catalonia, and partially funded by the Spanish Ministry of Science and Innovation (Grant No. AGL2016-76802-R to J.C) and the Research council of Norway (Grant 254872/E40 to R.N.F.). Participation of J.P. was financed by an award of the Biotechnology Overseas Associateship, Indian Ministry of Science and Technology.

Author contributions

Conceptualization, F.C. and J.C.; Methodology, F.C, J.P., C.D. and J.O.; Investigation, F.C., J.P., C.D. and J.O.; Writing - Original Draft, F.C.; Writing - Reviewing & Editing, R.N.F. and J.C.; Funding Acquisition, R.N.F. and J.C.; Resources, F.C., R.N.F. and J.C.; Supervision, J.C.

Conflict of interests

The authors declare no conflicts of interest associated with this manuscript.

References

Arrighi S, Aralla M (2014) Immunolocalization of aquaporin water channels in the domestic cat male genital tract. *Reprod Domes. Anim* **49**, 17-26.

Arrighi S (2014) Are the basal cells of the mammalian epididymis still an enigma? *Reprod Fertil Dev* **26**, 1061-1071.

Arrighi S, Bosi G, Accogli G, Desantis S (2016) Seasonal and ageing-depending changes of aquaporins 1 and 9 expression in the genital tract of buffalo bulls (*Bubalus bubalis*). *Reprod Domest Anim* **51**, 515-523.

Badran HH, Hermo LS (2002) Expression and regulation of aquaporins 1, 8, and 9 in the testis, efferent ducts, and epididymis of adult rats and during postnatal development. *J Androl* **23,** 358-373.

Belleannée C, Da Silva N, Shum WW, Marsolais M, Laprade R, Brown D, Breton S (2009) Segmental expression of the bradykinin type 2 receptor in rat efferent ducts and epididymis and its role in the regulation of aquaporin 9. *Biol Reprod* **80,** 134-143.

Billard R (1986) Spermatogenesis and spermatology of some teleost fish species. *Reprod Nutr Develop* **26,** 877-920.

Boj M, Chauvigné F, Cerdà J (2015a) Aquaporin biology of spermatogenesis and sperm physiology in mammals and teleosts. *Biol Bull* **229,** 93-108.

Boj M, Chauvigné F, Zapater C, Cerdà J (2015b) Gonadotropin-activated androgen-dependent and independent pathways regulate aquaporin expression during teleost (*Sparus aurata*) Spermatogenesis. *PLoS One* **10,** e0142512.

Boj M, Chauvigné F, Cerdà J (2015c) Coordinated action of aquaporins regulates sperm motility in a marine teleost. *Biol Reprod* **93,** 40.

Cerdà J, Finn RN (2010) Piscine aquaporins: an overview of recent advances. *J Exp Zool A Ecol Genet Physiol* **313,** 623-650.

Cerdà J, Chauvigné F, Finn RN (2017) The physiological role and regulation of aquaporins in teleost germ cells. *Adv Exp Med Biol* **969,** 149-171.

Chauvigné F, Boj M, Vilella S, Finn RN, Cerdà J (2013) Subcellular localization of selectively permeable aquaporins in the male germ line of a marine teleost reveals spatial redistribution in activated spermatozoa. *Biol Reprod* **89,** 37.

Chauvigné F, Boj M, Finn RN, Cerdà J (2015) Mitochondrial aquaporin-8-mediated hydrogen peroxide transport is essential for teleost spermatozoon motility. *Sci Rep* **5,** 7789.

Chauvigné F, Fjelldal PG, Cerdà J, Finn RN (2016) Auto-adhesion potential of extraocular aqp0 during teleost development. *PLoS One* **11,** e0154592.

Clemens DM, Németh-Cahalan KL, Trinh L, Zhang T, Schilling TF, Hall JE (2013) In vivo analysis of aquaporin 0 function in zebrafish: permeability regulation is required for lens transparency. *Invest Ophthalmol Vis Sci* **54,** 5136-5143.

Clulow J, Jones RC, Hansen LA, Man SY (1998) Fluid and electrolyte reabsorption in the ductuli efferentes testis. *J Reprod Fertil* **Suppl. 53,** 1-14.

Cooper **TG, Brooks DE** (1981) Entry of glycerol into the rat epididymis and its utilization by epididymal spermatozoa. *J Reprod Fertil* **61,** 163-169.

Cornwall GA, Horsten HH (2007) Sperm maturation in the epididymis. In: *The Genetics of Male Infertility*, Carrell DT, ed. Humana Press, Totowa, NJ, pp. 211-231.

582 **Da Silva N, Silberstein C, Beaulieu VV, Piétrement C, Van Hoek AN, Brown D, Breton S**
583 (2006a) Postnatal expression of aquaporins in epithelial cells of the rat epididymis. *Biol*
584 *Reprod* **74,** 427-438.
585 **Da Silva N, Piétrement C, Brown D, Breton S** (2006b) Segmental and cellular expression of
586 aquaporins in the male excurrent duct. *Biochim Biophys Acta* **1758,** 1025-1033.
587 **Da Silva N, Cortez-Retamozo V, Reinecker HC, et al** (2011) A dense network of dendritic cells
588 populates the murine epididymis. *Reproduction* **141,** 653-663.
589 **Dacheux JL, Dacheux F** (2013) New insights into epididymal function in relation to sperm
590 maturation. *Reproduction* **147,** R27-R42.
591 **Domeniconi RF, Orsi AM, Justulin LA, Leme Beu CC, Felisbino SL** (2008) Immunolocalization
592 of aquaporins 1, 2 and 7 in rete testis, efferent ducts, epididymis and vas deferens of adult
593 dog. *Cell Tissue Res* **332,** 329-335.
594 **Engelund MB, Chauvigné F, Christensen BM, Finn RN, Cerdà J, Madsen SS** (2013)
595 Differential expression and novel permeability properties of three aquaporin 8 paralogs from
596 seawater-challenged Atlantic salmon smolts. *J Exp Biol* **216,** 3873-3885.
597 **Fabra M, Raldúa D, Power DM, Deen PM, Cerdà J** (2005) Marine fish egg hydration is
598 aquaporin-mediated. *Science* **307,** 545.
599 **Finn RN, Chauvigné F, Hlidberg JB, Cutler CP, Cerdà J** (2014) The lineage-specific evolution
600 of aquaporin gene clusters facilitated tetrapod terrestrial adaptation. *PLoS One* **9,** e113686.
601 **Finn RN, Cerdà J** (2015) Evolution and functional diversity of aquaporins. *Biol Bull* **229,** 6-23.
602 **Finn RN, Cerdà J** (2016) Aquaporin. In: *Encyclopedia of Signaling Molecules*, 2nd Edition. Choi
603 S, ed. Springer, New York, pp 1-18.
604 **Ford JJr, Carnes K, Hess RA** (2014) Ductuli efferentes of the male Golden Syrian hamster
605 reproductive tract. *Andrology* **2,** 510-520.
606 **Hermo L, Krzeczunowicz D, Ruz R** (2004) Cell specificity of aquaporins 0, 3, and 10 expressed
607 in the testis, efferent ducts, and epididymis of adult rats. *J Androl* **25,** 494-505.
608 **Hermo L, Schellenberg M, Liu LY, Dayanandan B, Zhang T, Mandato CA, Smith CE** (2008)
609 Membrane domain specificity in the spatial distribution of aquaporins 5, 7, 9, and 11 in
610 efferent ducts and epididymis of rats. *J Histochem Cytochem* **56,** 1121-1135.
611 **Hermo L, Smith C** (2011) Thirsty business: cell, region, and membrane specificity of aquaporins
612 in the testis, efferent ducts, and epididymis and factors regulating their expression. *J Androl*
613 **32,** 565-575.
614 **Hess RA** (2002) The efferent ductules: structure and functions. In: *The Epididymis: From*
615 *Molecules to Clinical Practice*, Robaire B and Hinton BT, eds. Kluwer Academic/Plenum
616 Publishers. pp. 49-80.
617 **Huang HF, He RH, Sun CC, Zhang Y, Meng QX, Ma YY** (2006) Function of aquaporins in
618 female and male reproductive systems. *Hum Reprod Update* 12, 785-795.
619 **Inoue M, Wakayama Y, Kojima H, Shibuya S, Jimi T, Hara H, Iijima S, Masaki H, Oniki H,**
620 **Matsuzaki Y** (2009) Aquaporin 9 expression and its localization in normal skeletal myofiber.
621 *J Mol Histol* 40, 165-170.
622 **Kamsteeg EJ, Deen PM** (2001) Detection of aquaporin-2 in the plasmamembranes of oocytes: a
623 novel isolation method with improved yield and purity. *Biochem Biophys Res Commun* **282,**
624 683-690.
625 **King LS, Kozono D, Agre P** (2004) From structure to disease: the evolving tale of aquaporin
626 biology. *Nat Rev Mol Cell Biol* **5,** 687-698.
627 **Klein C, Troedsson MH, Rutllant J** (2013) Region-specific expression of aquaporin subtypes in
628 equine testis, epididymis, and ductus deferens. *Anat Rec (Hoboken)* **296,** 1115-1126.
629 **Kumari SS, Varadaraj K** (2009) Intact AQP0 performs cell-to-cell adhesion. *Biochem Biophys*
630 *Res Commun* **390,** 1034-1039.

Lahnsteiner F, Patzner RA, Weismann T (1993a) The spermatic ducts of salmonid fishes (Salmonidae, Teleostei). Morphology, histochemistry and composition of the secretion. *J Fish Biol* **42,** 79-93.

Lahnsteiner F, Patzner RA, Weismann T (1993b) The efferent duct system of the male gonads of the European pike (*Esox lucius*): testicular efferent ducts, testicular main ducts and spermatic ducts. *J Submicrosc Cytol Pathol* **25,** 487-498.

Lahnsteiner F, Patzner RA, Weismann T (1994) The testicular main ducts and spermatic ducts in cyprinid fishes. I. Morphology, fine structure and histochemistry. *J Fish Biol* **44,** 937-951.

Lahnsteiner F (2003) Morphology, fine structure, biochemistry, and function of the spermatic ducts in marine fish. *Tissue Cell* 35, 363-373.

Maeda N (2012) Implications of aquaglyceroporins 7 and 9 in glycerol metabolism and metabolic syndrome. *Mol Aspects Med* **33,** 665-675.

Marchissio MJ, Francés DE, Carnovale CE, Marinelli RA (2012) Mitochondrial aquaporin-8 knockdown in human hepatoma HepG2 cells causes ROS-induced mitochondrial depolarization and loss of viability. *Toxicol Appl Pharmacol* **264,** 246-254.

Meneguelli De Souza LC, Retamal CA, Rocha GM, Lopez ML (2015) Morphological evidence for a permeability barrier in the testis and spermatic duct of *Gymnotus carapo* (Teleostei: Gymnotidae). *Mol Reprod Dev* **82,** 663-678.

Melo RMC, Ribeiro YM, Luz RK, Bazzoli N, Rizzo E (2016) Influence of low temperature on structure and dynamics of spermatogenesis during culture of *Oreochromis niloticus. Animal Reprod Science* **172,** 148-156.

Miyauchi T, Yamamoto H, Abe Y, Yoshida GJ, Rojek A, Sohara E, Uchida S, Nielsen S, Yasui M (2015) Dynamic subcellular localization of aquaporin-7 in white adipocytes. *FEBS Lett* **589,** 608-614.

Nagahama Y (1983) The functional morphology of teleost gonads. In: *Fish Physiology* vol 9 pt A, Hoar WS, Randall DJ, Donaldson EM, ed. Academic Press, New York, pp 223-264.

Oliveira CA, Carnes K, França LR, Hermo L, Hess RA (2005) Aquaporin-1 and -9 are differentially regulated by oestrogen in the efferent ductule epithelium and initial segment of the epididymis. *Bio. Cell* **97,** 385-395.

Oliveira RL, Campolina-Silva GH, Nogueira JC, Mahecha GA, Oliveira CA (2013) Differential expression and seasonal variation on aquaporins 1 and 9 in the male genital system of big fruit-eating bat *Artibeus lituratus*. *Gen Comp Endocrinol* **186,** 116-125.

Pastor-Soler N, Isnard-Bagnis C, Herak-Kramberger C, Sabolic I, Van Hoek A, Brown D, Breton S (2002) Expression of aquaporin 9 in the adult rat epididymal epithelium is modulated by androgens. *Biol Reprod* **66,** 1716-1722.

Pastor-Soler NM, Fisher JS, Sharpe R, Hill E, Van Hoek A, Brown D, Breton S (2010) Aquaporin 9 expression in the developing rat epididymis is modulated by steroid hormones. *Reproduction* **139,** 613-621.

Robaire B, Hinton BT, Orgebin-Crist MC (2006) The epididymis. In: *Knobil and Neill's Physiology of Reproduction*, Vol. 1, Neill JD, Plant TM, Pfaff DW, Challis JRG, de Kretser DM, Richards JS, Wassarman P, eds. Elsevier Academic Press, St. Louis, MO. pp. 1071-1148.

Rojek AM, Skowronski MT, Füchtbauer EM, Füchtbauer AC, Fenton RA, Agre P, Frøkiaer J, Nielsen S (2007) Defective glycerol metabolism in aquaporin 9 (AQP9) knockout mice. Proc Natl Acad Sci U S A. **104,** 3609-3614.

Ruz R, Gregory M, Smith CE, Cyr DG, Lubahn DB, Hess RA, Hermo L (2006) Expression of aquaporins in the efferent ductules, sperm counts, and sperm motility in estrogen receptor-alpha deficient mice fed lab chow versus casein. *Mol Reprod Dev* **73,** 226-237.

Schulz RW, de França LR, Lareyre JJ, Le Gac F, Chiarini-Garcia H, Nobrega RH, Miura T (2010) Spermatogenesis in fish. *Gen Comp Endocrinol* **165,** 390-411.

Scott AP, Sumpter JP, Stacey N (2010) The role of the maturation-inducing steroid, 17,20-dihydroxypregn-4-en-3-one, in male fishes: a review. *J Fish Biol* **76,** 183-224.
Shum WW, Smith TB, Cortez-Retamozo V, et al (2014) Epithelial basal cells are distinct from dendritic cells and macrophages in the mouse epididymis. *Biol Reprod* **90,** 90.
Soria LR, Fanelli E, Altamura N, Svelto M, Marinelli RA, Calamita G (2010) Aquaporin-8-facilitated mitochondrial ammonia transport. *Biochem Biophys Res Commun* **393,** 217-221.
Tang V (2017) Cell-cell adhesion interface: rise of the lateral membrane. *F1000Res* **6,** 276.
Tingaud-Sequeira A, Chauvigné F, Fabra M, Lozano J, Raldúa D, Cerdà J (2008) Structural and functional divergence of two fish aquaporin-1 water channels following teleost-specific gene duplication. *BMC Evol Biol* **8,** 259.
Tingaud-Sequeira A, Calusinska M, Finn RN, Chauvigné F, Lozano J, Cerdà J (2010) The zebrafish genome encodes the largest vertebrate repertoire of functional aquaporins with dual paralogy and substrate specificities similar to mammals. *BMC Evol Biol* **10,** 38.
Turner TT (1995) On the epididymis and its role in the development of the fertile ejaculate. *J Androl* **16,** 292-298.
Verkman AS (2009) Knock-out models reveal new aquaporin functions. *Handb Exp Pharmacol* **190,** 359-381.
Walter I, Tschulenk W, Schabuss M, Miller I, Grillitsch B (2005) Structure of the seminal pathway in the European chub, *Leuciscus cephalus* (Cyprinidae); Teleostei. *J Morphol* **263,** 375-391.
Wang W, Hart PS, Piesco NP, Lu X, Gorry MC, Hart TC (2003) Aquaporin expression in developing human teeth and selected orofacial tissues. *Calcif Tissue Int* **72,** 222-227.
Wakayama Y, Hirako S, Ogawa T, Jimi T, Shioda S (2014) Upregulated expression of AQP 7 in the skeletal muscles of obese ob/ob mice. *Acta Histochem Cytochem* **47,** 27-33.
Zapater C, Chauvigné F, Norberg B, Finn RN, Cerdà J (2011) Dual neofunctionalization of a rapidly evolving aquaporin-1 paralog resulted in constrained and relaxed traits controlling channel function during meiosis resumption in teleosts. *Mol Biol Evol* **28,** 3151-3169.

710 **Table 1** Gilthead seabream-specific aquaporin antibodies used in the present study

Aquaporin	GenBank acc. No.	Antigenic peptide sequence [1]	Host	References
Aqp0a	AGT57405	AEGQQETRGEPIELKTQAL	Rabbit	Chauvigné et al. (2013)
Aqp1aa	AAV34610	PKFDDFPERMKVLVS	Rabbit	Raldúa et al. (2008), Chauvigné et al. (2013)
Aqp1ab	AAV34609	PREGNSSPGPSQGPSQWPKH	Rabbit	Fabra et al. (2005), Chauvigné et al. (2013)
Aqp3a	AGT57408	NVASNDNSLKATKEM	Chicken	Present study
Aqp4a	KY682700	SDPEKSEKKDLFQDSTGE	Chicken	Present study
Aqp7	AGT57406	LVEEETAPLGKKENI	Rabbit	Chauvigné et al. (2013)
Aqp8bb	ABK20159	LGDRKMRLILK	Rabbit	Chauvigné et al. (2013)
Aqp9b	AGT57407	PEKQEEKNVQDKYEI	Rabbit	Chauvigné et al. (2013)
Aqp10b	AAR13054	QEATEEKAGVELEGVK	Rabbit	Present study

711 [1] All sequences are in the cytoplasmic C-terminus of the predicted proteins.
712
713

Figures

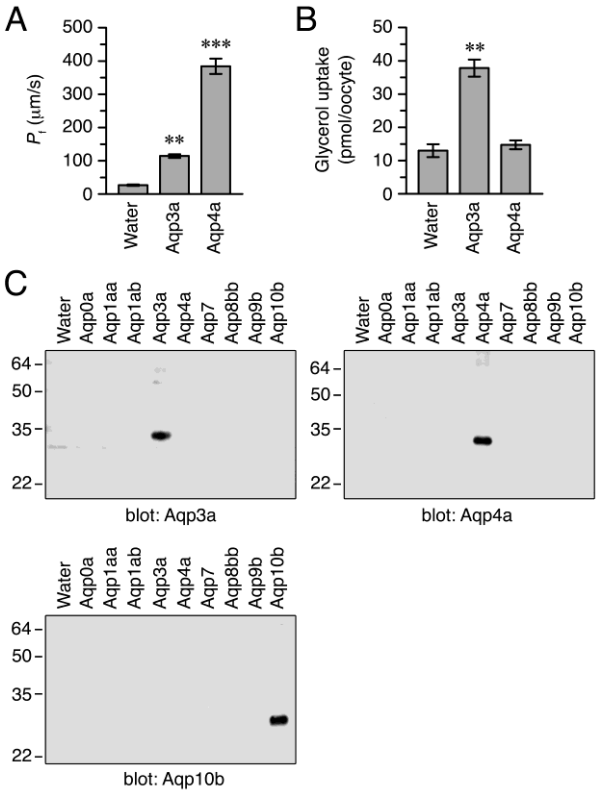

Fig. 1. Functional characterization of gilthead seabream Aqp3a and -4a and antibody specificity. Osmotic water permeability (P_f; A) and glycerol uptake (B) of *X. laevis* oocytes injected with water (control) or 15 ng of cRNA encoding Aqp3a or -4a. Data are the mean ± SEM (n = 10-15 oocytes). **, $P < 0.01$; ***, $P < 0.001$, with respect control oocytes. (C) Western blot of total membranes of *X. laevis* oocytes injected with water or expressing different seabream aquaporins. Three oocyte equivalents were loaded per lane. Membranes were probed with seabream specific antibodies against Aqp3a, -4 or -10b as indicated. Note that none of the antisera showed cross-reactivity with another aquaporin. Molecular mass markers (kDa) are on the left.

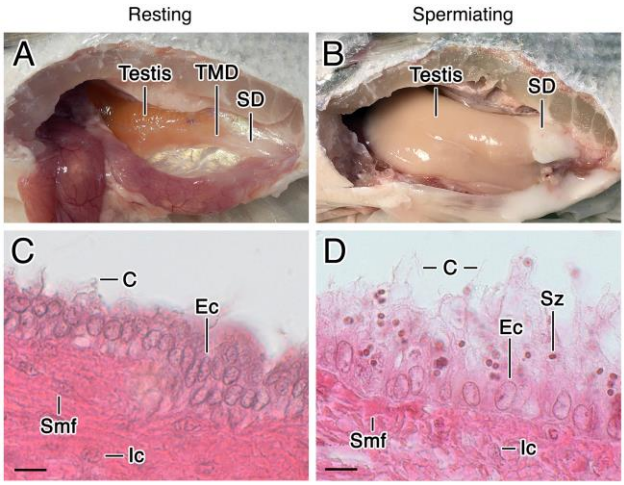

730
731
732 **Fig. 2.** Structure of the gilthead seabream spermatic duct. Photographs (A, B) and histological
733 sections stained with H&E (C, D) of the spermatic duct from males at the resting and spermiating
734 stage. Scale bars, 5 μm. TMD, testicular main duct; SD, spermatic duct; Ec, epithelial cell; C, cilia
735 (extended microvilli); Smf, smooth muscle fiber; Sz, spermatozoa; Ic, interstitial cell.
736
737

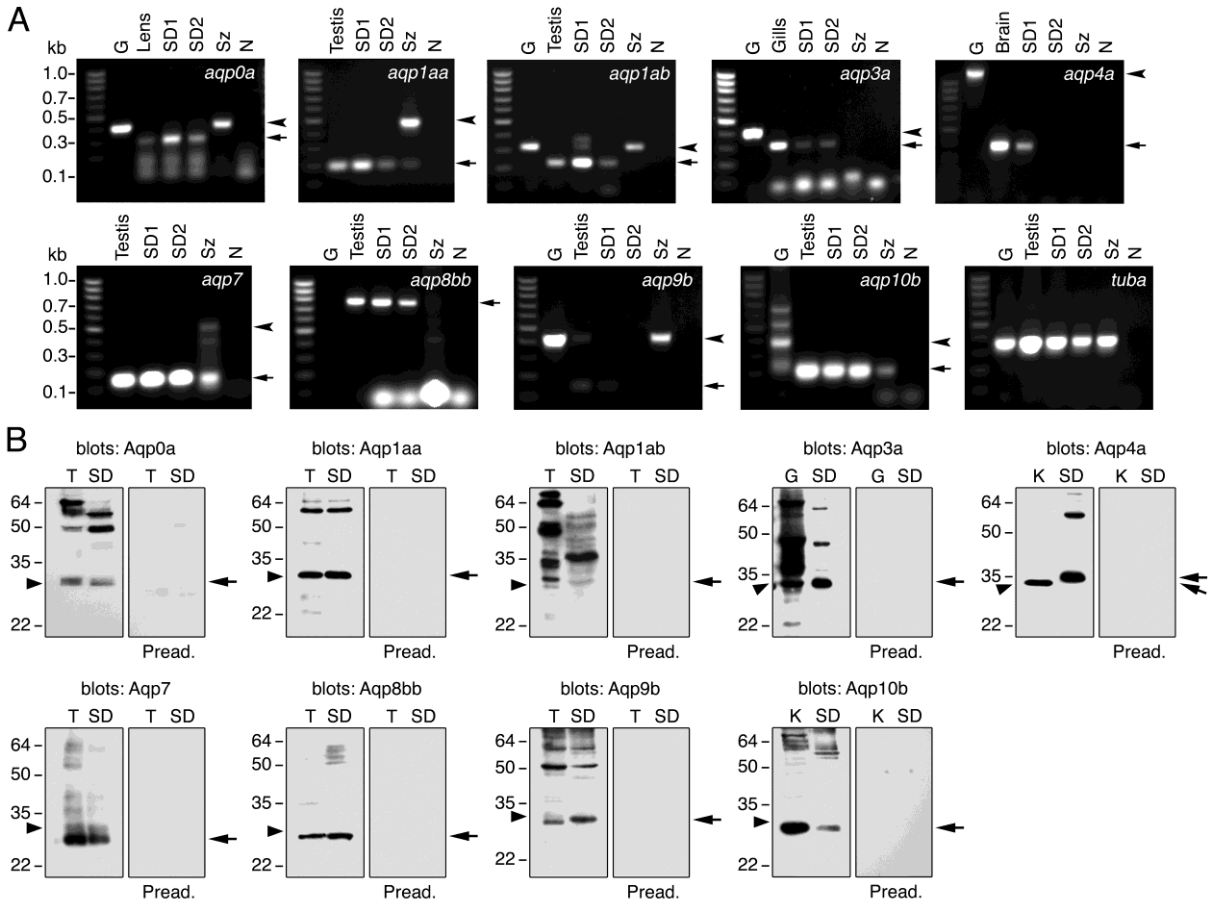

Fig. 3. RT-PCR and immunoblotting analysis of aquaporin expression in the gilthead seabream spermatic duct. (A) Representative RT-PCR analysis of aquaporin gene expression in the testis, lens, gills or brain (used as positive control tissues), spermatic duct from males at the resting and spermiating stages (SD1 and SD2, respectively), and spermatozoa (Sz). G, genomic DNA; N, negative control (absence of RT during cDNA synthesis). The arrows indicate transcripts, whereas the arrowheads indicate genomic products. The size (kb) of PCR products and molecular markers are indicated on the left. (B) Western blot analysis of aquaporins in seabream testis, gills or kidney (positive controls) and spermatic duct (SD) using paralog-specific antibodies. Duplicated blots were run in parallel where incubation was performed using primary antibodies that had been preadsorbed (Pread.) by the antigenic peptides to test for specificity. Arrows indicate aquaporin monomers and arrowheads the expected size of the target bands based on in silico determination of molecular masses. Molecular mass markers (kDa) are on the left.

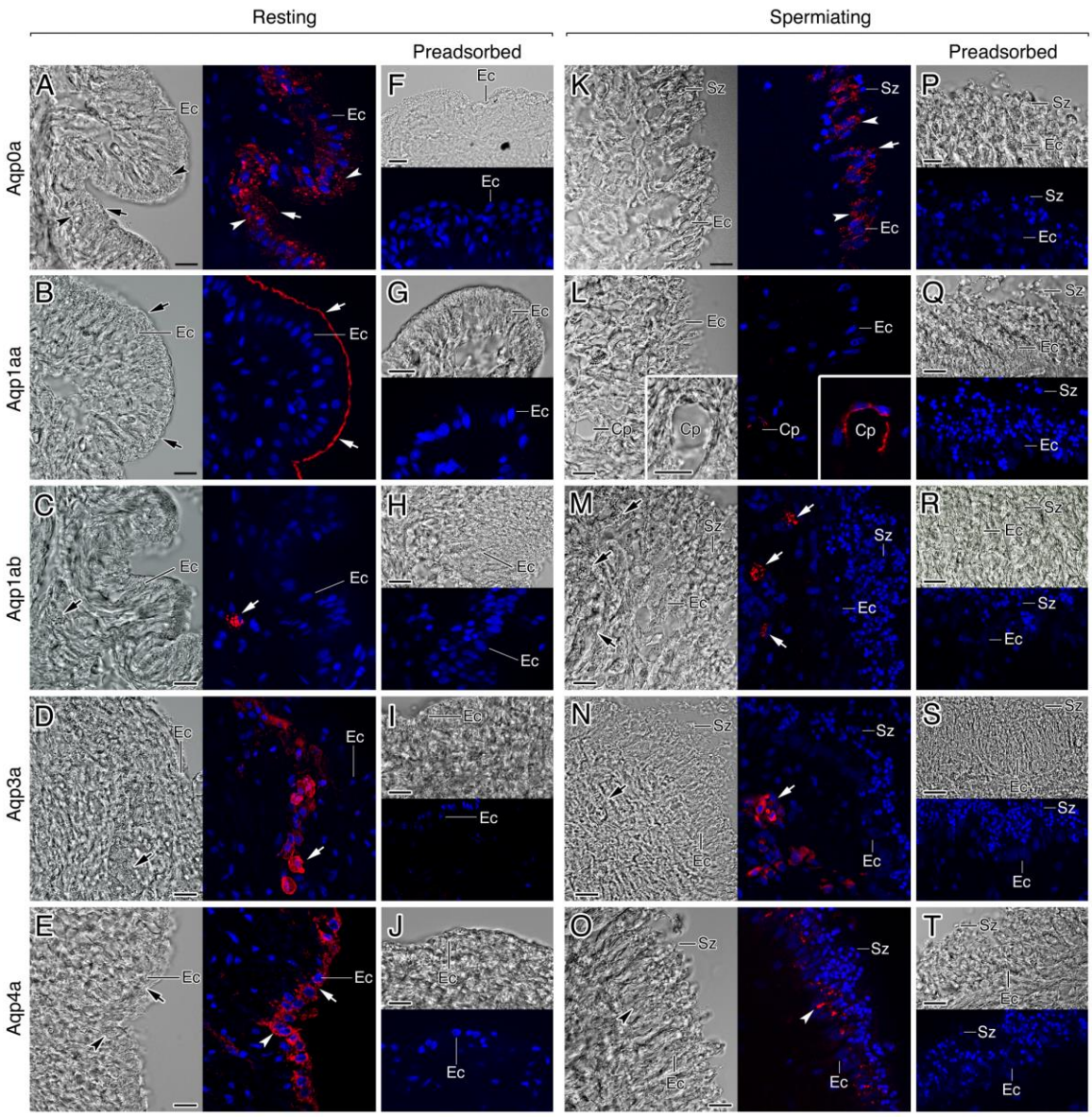

Fig. 4. Immunolocalization of Aqp0a, -1aa, -1ab, -3a and -4a in the gilthead seabream spermatic duct. Representative bright field (A-T, left and upper panels) and immunofluorescence microscopy images (A-T, right and lower panels) of Aqp0a (A and K), Aqp1aa (B and L), Aqp1ab (C and M), Aqp3a (D and N) and Aqp4a (E and O) localization in the spermatic duct of males at the resting and spermiating stage as indicated. Sections were labeled with affinity-purified rabbit or chicken polyclonal antibodies. The reactions were visualized with Cy3-conjugated sheep anti rabbit or chicken IgG (red) and the nuclei were counterstained with DAPI (blue). Control sections incubated with preabsorbed antisera were negative (F-J and P-T, lower panels). Scale bars, 10 µm. In panels A, B, E, K, L and O, arrows point to the plasma membrane, while the arrowheads indicate the cytoplasm. In panels C, D, M and N, the arrows point to the interstitial cells. Ec, epithelial cell; Cp, capillary; Sz, spermatozoa.

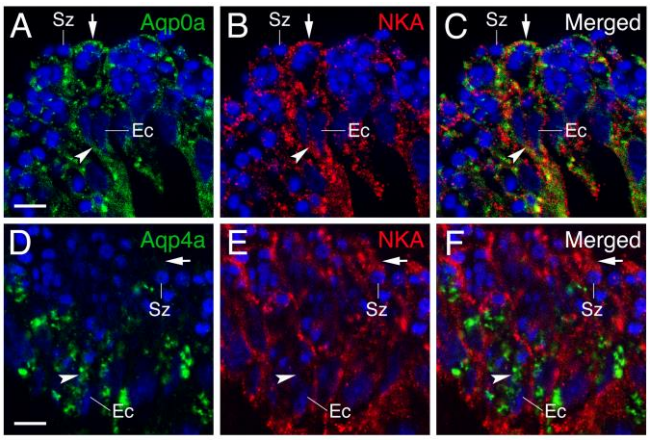

769
770
771 **Fig. 5.** Immunolocalization of Aqp0a and -4a with Na^+/K^+-ATPase (NKA) in the spermatic duct of
772 spermiating males. Epifluorescence photomicrographs showing double labeling for Aqp3a or -4a
773 (green) with NKA (red) (A-C and D-F, respectively) in the epithelial cells of the duct. In both
774 sections, the cell nuclei were stained with DAPI (blue). The fluorescence of different channels and
775 the merged images (C and F) shown were derived from the same section. Scale bars, 5 µm. The
776 arrows point to the plasma membrane, while the arrowheads indicate the cytoplasm. Ec, epithelial
777 cell; Sz, spermatozoa.
778
779

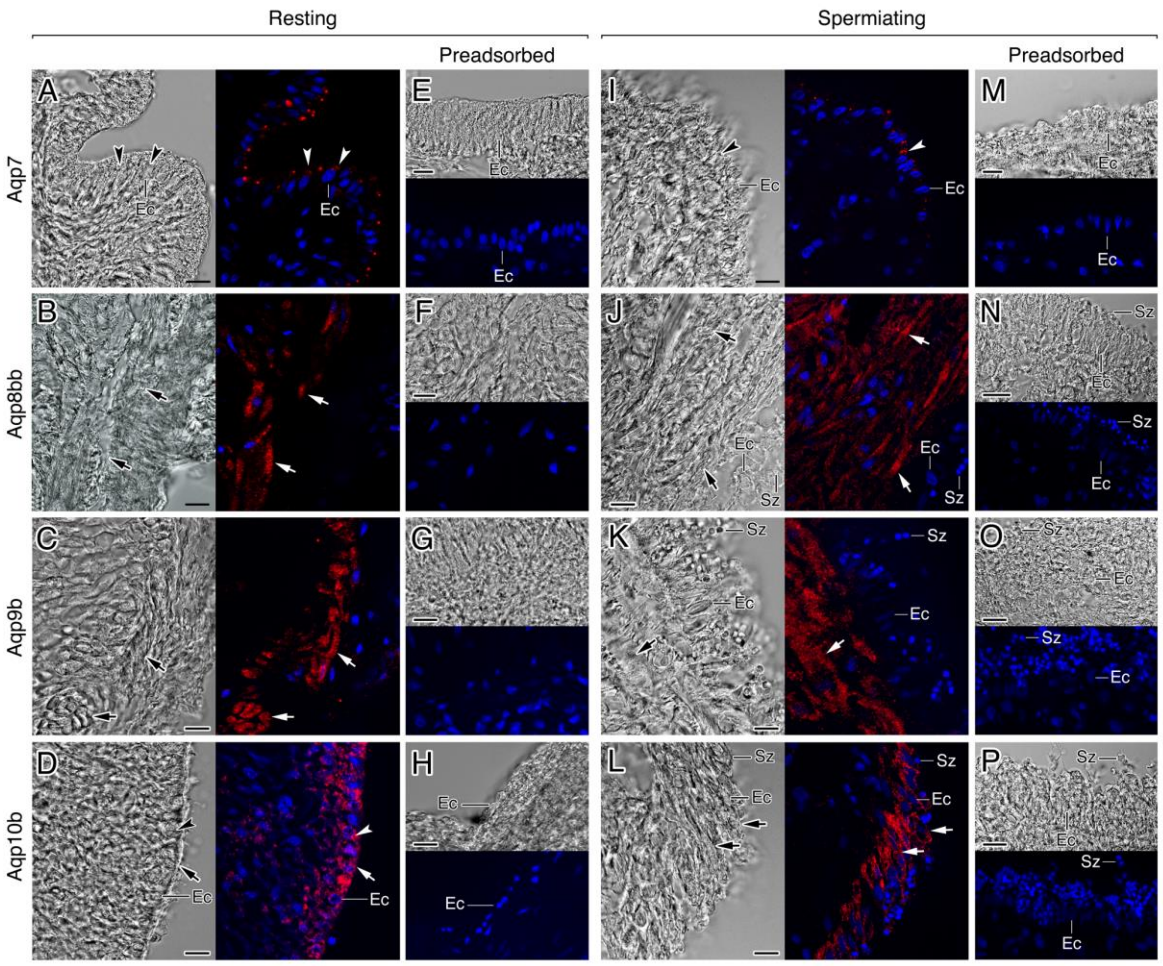

Fig. 6. Immunolocalization of Aqp7, -8bb, -9b, and -10b in the gilthead seabream spermatic duct. Representative bright field (A-P, left and upper panels) and immunofluorescence microscopy images (A-P, right and lower panels) of Aqp7 (A and I), Aqp8bb (B and J), Aqp9b (C and K), and Aqp10b (D and L) localization in the spermatic duct of males at the resting and spermiating stage as indicated. Sections were labeled with affinity-purified rabbit polyclonal antibodies. The reactions were visualized with Cy3-conjugated sheep anti rabbit IgG (red) and the nuclei were counterstained with DAPI (blue). Control sections incubated with preabsorbed antisera were negative (E-H and M-P). Scale bars, 10 μm. In panels A, I, D and L, arrows point to the plasma membrane, while the arrowheads indicate the cytoplasm. In panels B, J, C and K, the arrows point to the smooth muscle fibers. Ec, epithelial cell; Sz, spermatozoa.

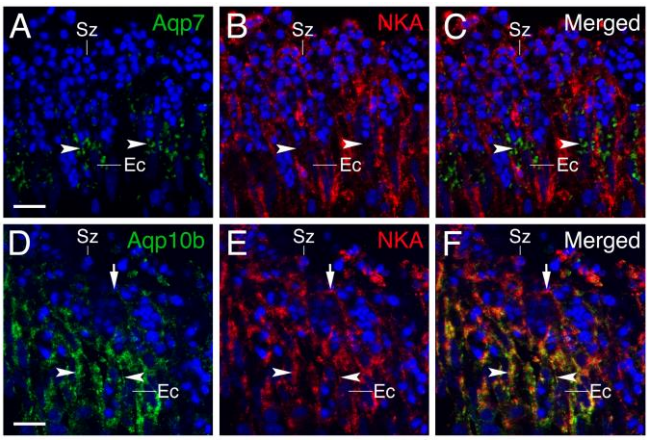

Fig. 7. Immunolocalization of Aqp7 and -10b with Na^+/K^+-ATPase (NKA) in the spermatic duct of spermiating males. Epifluorescence photomicrographs showing double labeling for Aqp7 or -10b (green) with NKA (red) (A-C and D-F, respectively) in the epithelial cells of the duct. In both sections, the cell nuclei were stained with DAPI (blue). The fluorescence of different channels and the merged images (C and F) shown were derived from the same section. Scale bars, 5 µm. The arrows point to the plasma membrane, while the arrowheads indicate the cytoplasm. Ec, epithelial cell; Sz, spermatozoa.

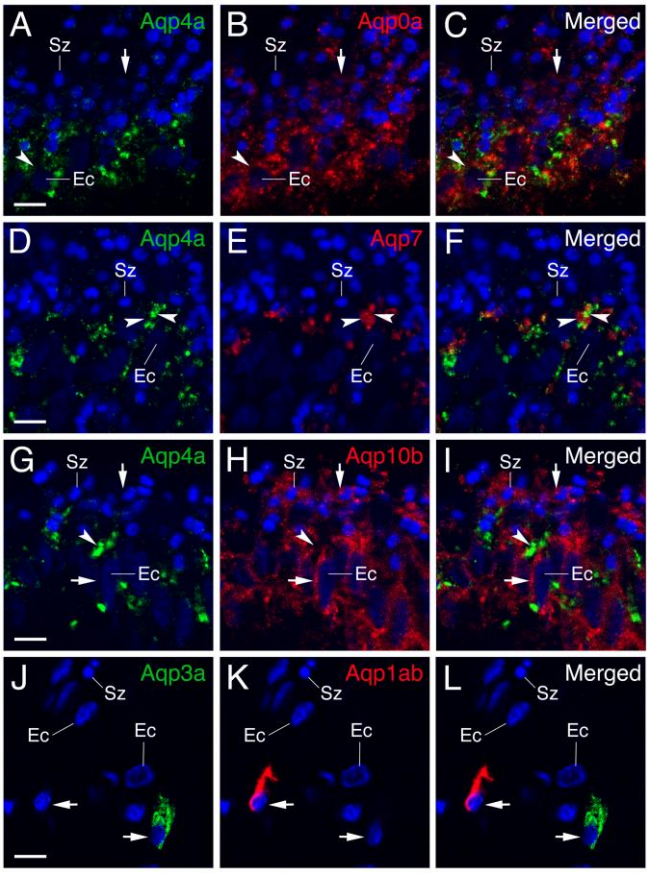

Fig. 8. Double immunostaining of Aqp4a with Aqp0a, -7 or -10b, and of Aqp3a with -1ab, in the spermatic duct of spermiating males. (A-I) Epifluorescence photomicrographs showing double labeling for Aqp4a (green) with Aqp0a (red; A-C), Aqp7 (red; D-F) or Aqp10b (red; G-I) in the epithelial cells of the duct. (J-L) Immunostaining of Aqp3a (green) and Aqp1ab (red) in some interstitial cells of the spermatic duct. In each section, the cell nuclei were stained with DAPI (blue). Scale bars, 5 µm. The arrows point to the plasma membrane, while the arrowheads indicate the cytoplasm. Ec, epithelial cell; Sz, spermatozoa.

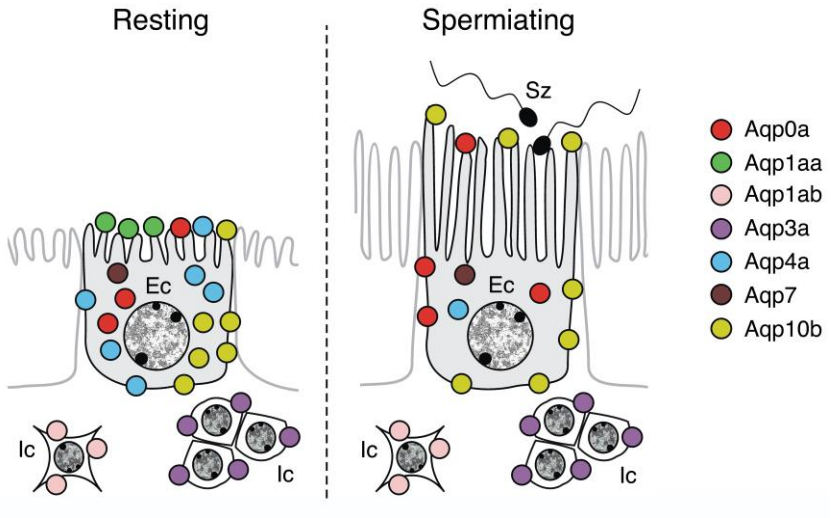

Fig. 9. Schematic diagram illustrating the changes in the subcellular distribution of aquaporins in the spermatic duct epithelium of the gilthead seabream during spermiation as revealed by the present study. At the resting stage, the epithelial cells express Aqp0a, -1aa, -4a, -7 and -10b. However, while Aqp1aa is exclusively distributed in the apical microvilli, Aqp4a and -10b are found intracellularly and in the apical and basolateral membranes, while Aqp7 is only found in the cytoplasm. Aqp0a also appears mainly in the cytoplasm but is also weakly detected in the apical microvilli. During spermiation, Aqp1aa is no longer expressed in the epithelial cells and Aqp4a seems to be internalized, whereas Aqp0a is expressed also in the lateral membrane in addition to the microvilli. In contrast, Aqp10b seems to be more accumulated in the apical and basolateral membranes of the epithelial cells than during the resting stage, whereas Aqp7 remains intracellular. Both during the resting and spermiation stages, different interstitial cells below the epithelium, not yet identified, express Aqp1ab or -3a, while Aqp8bb and -9b are expressed by the smooth muscle fiber cells (not shown).